

## **Experiments and MAAP4 Assessment for Core Mixture Level Depletion After Safety Injection Failure During Long-Term Cooling of a Cold Leg LB-LOCA**

**Y. S. Kim, B. U. Bae, G. C. Park, K. Y. Suh, and U. C. Lee**

Seoul University  
San56-1 Shilnlim, Kwanak, Seoul, Korea  
kysoo1@snu.ac.kr

(Received July 31, 2002)

### **Abstract**

Since DBA(Design Basis Accidents) has been studied rather separately from SA(Severe Accidents) in the conventional nuclear reactor safety analysis, the thermal hydraulics during transition between DBA and SA has not been identified so much as each accident itself. Thus, in this study, the thermal hydraulic behavior from DBA to the commencement of SA has been experimentally and analytically investigated for the long-term cooling phase of LB-LOCA(Large-Break Loss-of-Coolant Accident). Experiments were conducted for both cases of the loop seal open and closed in an integral test loop, named as SNUF (Seoul National University Facility), which was scaled down to 1/6.4 in length and 1/178 in area of the APR1400 (Advanced Power Reactor 1400MWe). The core mixture level was a main measured value since it took major role in the fuel heat-up rate, the location of fuel melting initiation and the channel blockage by melting material during SA. Experimental results were compared to MAAP4.03 to assess its model of calculating the core mixture level. MAAP4.03 overestimates the core two-phase mixture level because sweep-out and spill-over and the measures to simulate the status of loop seal are not included, which is against the conservatism. Thus, it is recommended that MAAP4.03 should be improved to simulate the thermal hydraulic phenomena, such as sweep-out, spill-over and the status of loop seal.

**Key Words** : APR1400, LB-LOCA, core mixture level, MAAP4, sweep-out

### **1. Introduction**

In the conventional nuclear reactor safety analysis, DBA (Design Basis Accidents) analysis has been studied rather separately from SA(Severe Accidents) analysis involving fuel melting. The

DBA analysis has been performed in the respect of the peak clad temperature (PCT). Many models to simulate the thermal hydraulic phenomena during DBA were developed and implanted in the DBA analysis codes, such as RELAP [1]. In general, the DBA analysis is terminated after all

the fuel rods are quenched after hitting PCT. On the other hand, the SA analysis focuses on the fuel degradation, melting and relocation from the moment when the core is uncovered with the safety injection (SI) failure. The effort to understand the SA phenomena has been made after TMI-2 accident and there was much progress in this area itself. However, the thermal hydraulic and fuel performance phenomena during transition between DBA and SA have not been identified so much as each accident itself and still defy fully comprehensive understanding. Also, these days, the best estimate method has been tried to apply to reduce inordinate conservatism to both DBA and SA analysis and the code development of one-through calculation from the initiation of DBA to core melting of SA such as SCDAP/RELAP5 [2] has been performed.

This study is part of DBA and SA combined analysis method development research. As the first part of this research, we investigated experimentally and analytically the thermal hydraulics after SI failure during the long-term cooling phase of LB-LOCA (Large-Break Loss-of-Coolant Accident) in the cold leg, particularly the depletion of core coolant inventory, which affect the fuel heat-up rate, the location of fuel melting initiation and the channel blockage by melting material. And, results from this study will be used in succeeding research of fuel heat-up and melting as initial and boundary conditions.

LB-LOCA was selected as a reference accident on the basis that this accident has relatively high CDF (Core Damage Frequency) if occurred, according to PSA results of APR1400 (Advanced Power Reactor 1400MWe) [3]. And, the integral test loop, named as SNUF (Seoul National University Facility) was built to be scaled down to 1/6.4 in length and 1/178 in area of the APR1400 [3] according to the three level scaling method [4, 5, 6]. Experiments were performed for

both cases of loop seal open and closed to include all of plant status expected to exist during transition from DBA to SA caused by safety injection pump failure after two hours elapsed from accident initiation.

MAAP4.03 [7], devoted to the SA analysis, calculates the depletion of core coolant inventory in simple method of only considering the coolant evaporation by the fuel submerged below the core two-phase mixture level. In actual, the multi-dimensional thermal hydraulic phenomena such as sweep-out and spill-over may accelerate the depletion of core coolant inventory. Since the sweep-out and the measures to simulate the status of loop seal are not included in the core inventory calculation of MAAP4.03, the core two-phase mixture level may potentially be overestimated against the conservatism required for the analysis in MAAP4.03 during the transients dealt with in this study. Thus, we evaluated the core inventory calculation method of MAAP4.03 through comparing the estimated of MAAP4.03 with the experimental results.

## 2. Selection of Experiment Scenario

According to the probabilistic safety assessment (PSA) results of the APR1400 [3], the core damage frequency (CDF) of LB-LOCA ranks the fifth among the considered accidents due to the low probability of the initiating event. However, since LB-LOCA has high CDF during transient if occurred as shown in Table 1, LB-LOCA is selected as a reference accident.

According to the component failure PSA results of the Safety Injection System (SIS) for LB-LOCA in APR1400 as shown in Table 2 [3], it is highly probable that all 4 MOV (Motor-Operated Valve) simultaneously fails to open on the SI actuation signal after the initiation of LB-LOCA. Even if the related components of safety injection pump are

**Table 1: PSA results for APR1400 [3]**

| Initial Event                | Initial Event Frequency (a) | Core Damage Frequency (b) | CDF/IEF (b/a) |
|------------------------------|-----------------------------|---------------------------|---------------|
| Station Blackout             | 1.24E-05                    | 1.21E-06                  | 9.76E-02      |
| Large LOCA                   | 6.97E-05                    | 6.91E-07                  | 9.91E-03      |
| Medium LOCA                  | 1.40E-04                    | 6.10E-07                  | 4.36E-03      |
| Small LOCA                   | 3.00E-03                    | 1.36E-06                  | 4.53E-04      |
| Steam Generator Tube rupture | 4.50E-03                    | 7.05E-07                  | 1.57E-04      |
| Loss of Main Feed-water      | 1.70E-01                    | 1.25E-06                  | 7.35E-06      |

**Table 2: PSA results of Safety Injection System for LB-LOCA in APR1400 [3]**

| Components            | Cause of Failure | Failure Frequency | Common Cause Failure Frequency |
|-----------------------|------------------|-------------------|--------------------------------|
| Safety Injection Pump | Starting Failure | 1.3E-3/day        | 4.84E-5/yr                     |
|                       | Running Failure  | 5.0E-5/hr         | 5.97E-5/yr                     |
| Check Valve<br>MOV    | Fail to open     | 2.0E-4/day        | 2.81E-5/yr                     |
|                       | Fail to open     | 4.0E-3/day        | 1.38E-4/yr                     |

inoperable, safety injection water can be supplied to about 200.0sec by SIT(Safety Injection Tank) equipped with Fluidic Device. In order to simulate plant conditions when SI is terminated due to SIT empty and MOV open failure, the heater power of 337.0kW is required in the our test facility-SNUF according to the scaling analysis, which corresponds to the decay heat of 156.0MW in the APR1400. Since there is the limitation in space for the electrical heaters installed in SNUF, the case of "all MOV fails to open" cannot be accommodated in SNUF. As an alternative on the basis of failure frequency in Table 2, we selected the case in which all SIPs' failure take place at two hours after the initiation of LB-LOCA as a Safety Injection Pumps (SIPs) running failure.

### 3. Design of Test Facility

#### 3.1. Initial Conditions of APR1400 and SNUF

The initial condition of experiment is the plant

state of long-term cooling phase, two hours elapsed from the initiation of LB-LOCA in cold leg, and determined based on the results of MARS2.1 [8] analysis for APR1400. According to the analysis results of MARS2.1, the core power is about 42.0 MWth(Fig. 1). The system pressure is about 0.18MPa close to containment pressure(Fig. 2). The coolant is saturated in two hot legs and in the cold legs of intact loop(Figs. 3 and 4) and subcooled about 8.7°C in the lower plenum(Fig. 5). The steam generator secondary side is saturated on the pressure of 0.17MPa(Fig. 6).

There are some differences in initial condition between APR1400 and SNUF as shown in Table 3. In the primary side, the difference of system pressure and temperature induced below 1% deviation in the properties such as specific heat and density. And, the difference of subcooling only gives rise to small time discrepancy in reaching saturation condition of core coolant. But, it scarcely affect the depletion of core two-phase mixture level because it is dominated by coolant

**Table 3. Initial Conditions in APR1400 and SNUF**

| Parameters                  | APR1400 [3]        | SNUF               |
|-----------------------------|--------------------|--------------------|
| Upper Plenum Pressure       | 0.18 MPa           | 0.1 MPa            |
| Lower Plenum Temperature    | 108.0 °C           | 95.0 °C            |
| Subcooling in Lower Plenum  | 8.7 °C             | 5.0 °C             |
| Core Exit Void Fraction     | 100 %              | 100 %              |
| Core and Downcomer Level    | Bottom of cold leg | Bottom of cold leg |
| Core Power                  | 42.0 MW            | 90.0 kW            |
| Steam Generator Pressure    | 0.17 MPa           | 0.2 MPa            |
| Steam Generator Temperature | 114.8 °C           | 120 °C             |

evaporation, spill-over and sweep-out after coolant reaching the saturation condition.

In the secondary side, after two hours elapsed from the initiation of LB-LOCA, there is no

noticeable heat transfer through steam generator tubes because thermal hydraulic conditions of primary and secondary side are maintained similarly. From these results, we can conclude that

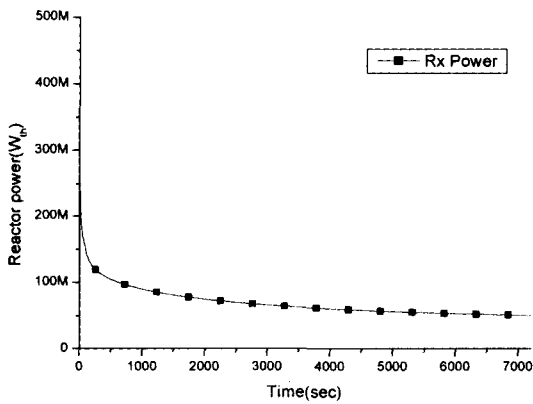


**Fig. 1. Reactor Power**

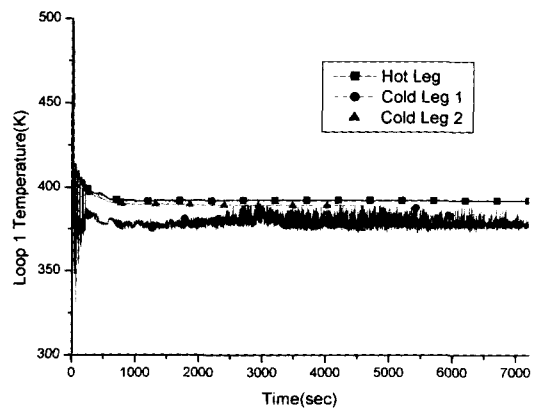


**Fig. 3. Loop 1 Coolant Temperature**

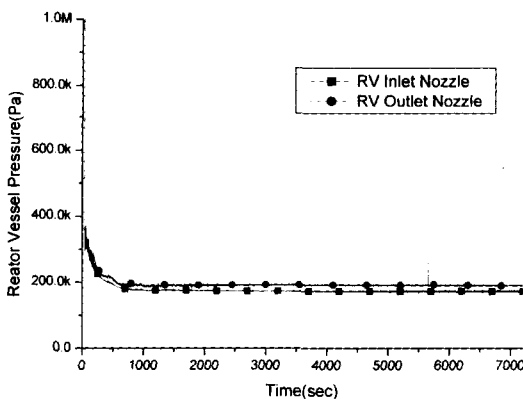


**Fig. 2. Reactor Vessel Pressure**

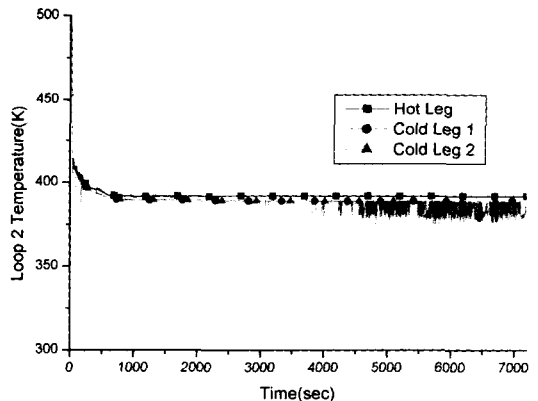


**Fig. 4. Loop 2 Coolant Temperature**

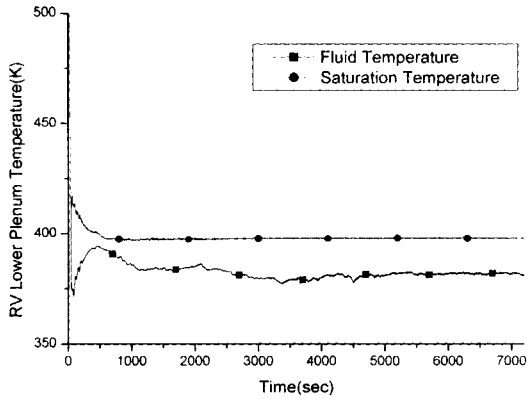


Fig. 5. Lower Plenum Temperature

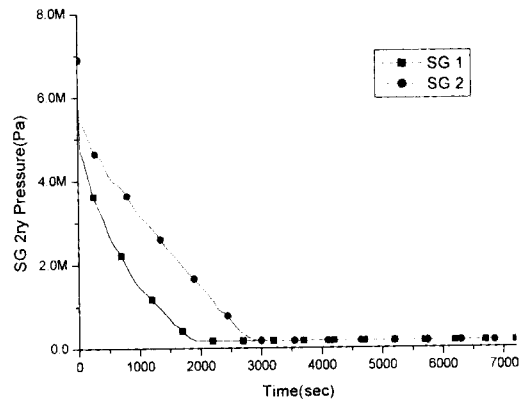


Fig. 6. Steam Generator Secondary Side Pressure

the difference of initial conditions between APR1400 and SNUF does not make a significant distortion in the experiment.

### 3.2. Scaling of Test Facility

The three-level scaling law was adopted to design of SNUF [4,5,6]. This law consists of the top-down and the bottom-up approaches to account for the global scaling, the boundary flow scaling and the local phenomena scaling. In the global scaling, the dimensionless numbers for the kinematic, dynamic and energetic similarities are

produced by the nondimensionalization of the governing equations as follows [4,5,6]:

Phase change number:

$$N_{pch} \equiv \left[ \frac{4q_0''' \delta l_0}{du_0 \rho_f i_{fg}} \right] \left[ \frac{\Delta p}{\rho_g} \right] \quad (1)$$

Subcooling Number:

$$N_{sub} \equiv \left[ \frac{i_{sub}}{i_{fg}} \right] \left[ \frac{\Delta p}{\rho_g} \right] \quad (2)$$

Froude number:

$$(N_{Fr})_R \equiv \left[ \frac{u_0^2}{gl_0 \alpha_0} \right]_R \left[ \frac{\rho_f}{\Delta p} \right]_R \quad (3)$$

Table 4: Design values for APR1400 and SNUF

| Parameter               |        | Unit           | APR1400 [3]           | SNUF                     | Ratio   |
|-------------------------|--------|----------------|-----------------------|--------------------------|---------|
| Vessel                  | Height | m              | 13.942                | 2.178                    | 1/6.4   |
|                         | Area   | m <sup>2</sup> | 13.3                  | 0.0748                   | 1/177.9 |
| Hot leg                 | Length | m              | 4.298                 | 0.672                    | 1/6.4   |
|                         | Area   | m <sup>2</sup> | 0.89                  | 4.999 × 10 <sup>-3</sup> | 1/178.0 |
| Cold leg                | Length | m              | 7.608                 | 1.189                    | 1/6.4   |
|                         | Area   | m <sup>2</sup> | 0.46                  | 2.579 × 10 <sup>-3</sup> | 1/178.4 |
| Break area              | Area   | m <sup>2</sup> | 0.46                  | 1.019 × 10 <sup>-3</sup> | 1/451.2 |
| Fuel hydraulic diameter |        | mm             | 11.97                 | 56.2                     | 1/0.213 |
| Fuel conduction depth   |        | mm             | 2.4                   | 5.0                      | 1/0.48  |
| Active core length      |        | m              | 3.81                  | 0.72                     | 1/5.29  |
| Heater power            |        | kW             | 4.2 × 10 <sup>4</sup> | 96.0                     | 1/437.5 |

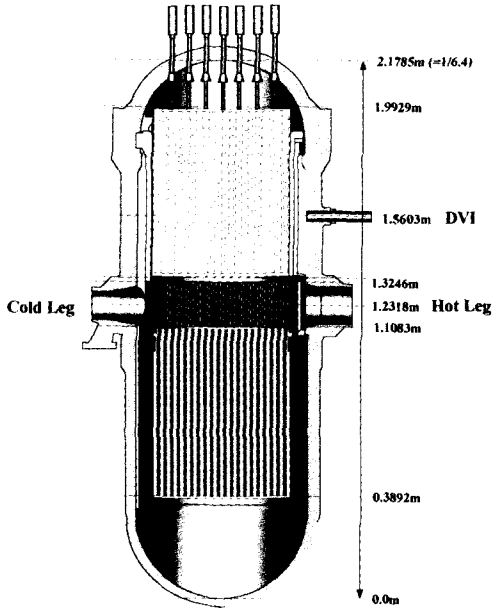


**Fig. 7. Cross-sectional Front View of SNUF Reactor Vessel**

Drift-flux number:

$$N_{df} \equiv \left[ \frac{V_{gj}}{u_0} \right]_i \quad (4)$$

Time ratio number:

$$T_i^* \equiv \left[ \frac{l_0/u_0}{\delta^2/\alpha_s} \right]_i \quad (5)$$

Thermal inertia ratio:

$$N_{thi} \equiv \left[ \frac{\rho_s c_{ps} \delta}{\rho_f c_{pf} d} \right]_i \quad (6)$$

Friction number

$$N_{fi} \equiv \left[ \frac{fl}{d} \right]_i \left[ \frac{1 + x(\Delta\rho/\rho_g)}{(1 + x(\Delta\mu/\mu_g))^{0.25}} \right] \left[ \frac{a_0}{a_i} \right]^2 \quad (7)$$

Orifice number:

$$N_{oi} \equiv K_i \left[ 1 + x^{3/2} (\Delta\rho/\rho_g) \right] \left[ \frac{a_0}{a_i} \right]^2 \quad (8)$$

In addition to above physical similarity groups, the

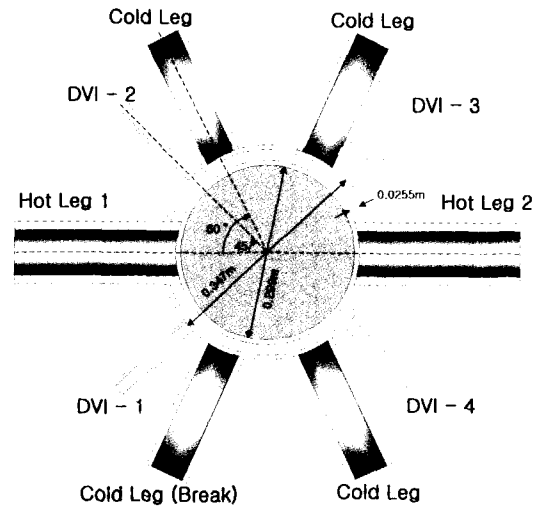


**Fig. 8. Cross-sectional Top View of SNUF Reactor Vessel**

geometric similarity groups are given as follows:

$$\begin{aligned} \text{Axial length scaling} &: L_i \equiv l_i/l_0 \\ \text{Flow area scaling} &: A_i \equiv a_i/a_0 \end{aligned} \quad (9)$$

The geometric scaling criterion requires the following relations to be satisfied for all the components of system:

$$\begin{aligned} L_{iR} &= (l_i/l_0)_R = 1 \\ A_{iR} &= (a_i/a_0)_R = 1 \end{aligned} \quad (10)$$

According to the requirements of Eq. (10), SNUF was scaled down 1/6.4 in length and 1/178 in area of APR1400 as shown in Figs. 7 and 8. The important geometrical design parameters of APR1400 and SNUF are shown in Table 4.

The hydraulic diameter and the conduction depth in the fuel and the heater are defined as follows:

$$d_i \equiv 4a_i/\xi_i \quad (11)$$

$$\delta_i \equiv a_{si}/\xi_i \quad (12)$$

where  $a_i$ ,  $a_{si}$  and  $\xi_i$  are the flow cross sectional area, the solid structure cross sectional area and the wetted perimeter of the heat structure in the

core, respectively. Hence,  $d_i$  and  $\delta_i$  are related by

$$d_i \equiv 4(a_i / a_{ii})\delta_i \quad (13)$$

In order to conserve the similarity between the prototype and the test facility, it is necessary to satisfy the following ratio of the value of a model to that of prototype for the similarity groups listed above:

$$\psi_R \equiv \frac{\psi_m}{\psi_p} \quad (14)$$

This experiment intends to measure the depletion of core two-phase mixture level. Thus, the similarity of the parameters affecting the core two-phase mixture level has to be preserved. The important nondimensional parameter is Froude number, which decides the core two-phase flow regime, and the void fraction of mixture in the core [9].

$$(N_{Fr})_R \equiv \left[ \frac{u_0^2}{g l_0 \alpha_0} \right]_R \left[ \frac{\rho_f}{\Delta \rho} \right]_R = \frac{(u_0^2)_R}{(l_0)_R} = 1 \quad (15)$$

According to the MARS2.1 analysis results for the plant state at two hours after the commencement of LB-LOCA in APR1400, the system pressure is nearly 0.18MPa; the subcooling about 8.7°C in the lower plenum. Since the test facility can be maintained on the similar thermal hydraulic conditions to the prototype, the fluid properties are conserved nearly same between the prototype and the test facility by using the same working fluid. Hence, the ratio of reference velocity,  $u_{0R}$  and that of length,  $l_{0R}$  are related by

$$u_{0R} = l_{0R}^{1/2} \quad (16)$$

The similarity in the drift flux number requires the following void relation to be satisfied

$$(\alpha_c)_R \left[ \frac{\Delta \rho}{\rho_f} \right]_R = 1 \quad \text{or} \quad (\alpha_c)_R \equiv 1 \quad (17)$$

Since the core exit void fractions are the same

as 1.0 in both prototype and test facility, the requirement of Eq. (17) is satisfied.

The orifice number is composed of the loss coefficient, the properties of fluid and the geometrical ratio. The ratio of the loss coefficient can be set equal to 1.0 when the area ratio among the system components is kept constant. Since the similar temperature and pressure are maintained in both the prototype and the model, the properties are nearly same. Thus, the similarity of the orifice number is conserved.

The similarity of the friction number in Eq. (7) leads to the following requirement:

$$f_R \approx l_R / d_R = 2.1 \quad (18)$$

For a given geometry and velocity, Reynolds number of the prototype can be calculated for the saturated steam condition as follows:

$$\begin{aligned} Re_p &= 3.072 \times 10^6 \\ Re_R &= \frac{\rho_R u_{0R} D_R}{\mu_R} \\ Re_m &= Re_p \times (u_{0R} D_R) = 7.5 \times 10^3 \end{aligned} \quad (19)$$

Using Reynolds numbers for the prototype and the test facility and the Moody chart of commercial wall condition[10], the friction factors were  $f_m \approx 0.03$  for the test facility,  $f_p \approx 0.01$  for the prototype and the ratio of friction factor,  $f_R$  was about 3.0. Therefore, the similarity of friction factor is nearly satisfied.

Since the subcooling number consists of the fluid properties, similarity is achieved by maintaining the similar temperature and pressure between the prototype and the test facility.

The thermal inertia number is defined as the ratio of the heat capacity of working fluid and the structure. Since the temperature of the structure is close to that of the fluid at two hours after the LB-LOCA initiation, the heat addition to the fluid from the structure is negligible in the experiment.

The phase change number in Eq. (1) is the

important dimensionless number since the phase change governs the steam generation rate, the quality in the core and the pressure behavior. The steam generation rate determines the steam velocity incoming to the downcomer, which determines the amount of sweep-out through interacting with the coolant in the downcomer. And, the quality directly affects to the two-phase mixture level in the core. The pressure behavior may produce the differential pressure between core and downcomer, which determines the amount of spill-over. Since the test facility can be maintained on the similar thermal hydraulic conditions to the prototype, the fluid properties are nearly same. Thus, we can get the power ratio from the phase change number ratio of Eq. (1) as follows:

$$[q_o]_R = \left[ \frac{\rho_g}{\Delta\rho} \right]_R \left[ \frac{du_o}{\alpha_o} \right]_R = 2.452 \quad (20)$$

Thus, total heat generation ratio can be calculated as follows:

$$[q_o]_R = [q_o]_R \times V_R = 2.152 \times 10^{-3} \quad (21)$$

Since the test condition corresponds to the plant state at two hours after the LB-LOCA initiation, the decay heat of the prototype is 42.0MWth pursuant to the decay heat model of the ANS-1979 [11]. The required total heater power of the test facility was determined as follows:

$$\begin{aligned} (q_o)_m &= (q_o)_P \times [q_o]_R = 42,000 \times 2.152 \times 10^{-3} \\ &= 90.4(\text{kW}) \end{aligned} \quad (22)$$

Although the heater power of 90.4kW was calculated by the similarity relation of Eq. (22), the heater power was designed to 96.0kW to consider the operation margin and the sensitivity study.

The time ratio number is calculated as follows:

$$\tau_R = \frac{(l_o)_R}{(u_o)_R} = (l_o)_R^{1/2} \quad (23)$$

This implies that if the axial length is reduced, the time events in the scaled-down model are accelerated by a factor of  $(l_o)_R^{1/2}$ . Since the length ratio between the test facility and the prototype is 1/6.4, the time ratio of the test facility is 0.395 from Eq. (23). Therefore, the transient in the test facility proceeds 2.5 times faster than the prototype.

The reference void fraction in Froude number of Eq. (3) is given by

$$\alpha_o = \left[ \frac{\rho_f}{\Delta\rho} \right] \left[ \frac{l}{1 + (N_d + 1)/(N_{pch} - N_{sub})} \right] \quad (24)$$

This value is automatically satisfied because the constituent nondimensional numbers have been conserved as mentioned above and the test facility is maintained at similar temperature and pressure to the prototype.

In the second-level scaling of the boundary flow and inventory scaling, the important parameter is the break flow that must satisfies the following relations:

$$(a_{break})_R = (l_o)_R^{1/2} (a_o)_R = 0.395 \times (a_o)_R \quad (25)$$

In order to keep the required break area, two orifices were installed in the break locations.

In the energy inventory scaling, the following relation must be considered

$$\frac{dE}{dt} = q - w + \sum m_{in} i_{in} - \sum m_{out} i_{out} \quad (26)$$

It can be seen from Eq. (26) that only the total heat without considering the heat addition mechanism is treated. When the heat addition from structure except fuel needs to be considered, it can be compensated with the increase of heater power as much as the heat addition from structure. However, as previously described, the heat addition from structure is negligible in this experiment.

The third-level scaling is the local phenomena



scaling. The major phenomenon of this study is sweep-out in the downcomer, which governs the coolant level in the core and the downcomer. This phenomenon can be preserved through conserving the flow regime of the prototype. The related parameters are the void fraction, the steam temperature and Froude number, which governs the behavior on the free surface [9]. The similarity of the void fraction has already been ascertained in Eq. (24) and the steam temperature ratio has been satisfied due to the similar pressure and temperature conditions between the prototype and the test facility. The similarity of Froude number has also been checked in Eq. (15). Thus, the similarity for sweep-out in the downcomer is conserved in the test facility. The major design parameters of the SNUF determined from the above similarity analysis are shown in Table 4 and compared with those of the APR1400.

**3.3. Description of SNUF**

The design parameters of SNUF based on the scaling study are shown in Figs. 7, 8 and Table 4. The test facility consists of one hot leg and two

cold legs in each loop as shown in Fig. 9. The reactor vessel contains 24 heaters to simulate the core decay heat of the prototype. The steam generator is equipped in each loop and each contains sixteen U-tubes. The DVI (Direct Vessel Injection) lines are connected to the upper reactor vessel as illustrated in Figs. 7, 8 and 9. The broken cold leg was designed to simulate the double-ended guillotine break between the reactor coolant pump and the reactor vessel by two broken section valves and one separation valve. Two discharge tanks connected to the broken section simulate the containment and measure the break flow with the level gauge equipped in the tank.

As shown in Fig. 10, the core two-phase mixture level is measured with the float type level transmitter equipped with the reed switches in the tube; the downcomer liquid level with the DP (differential pressure) transmitter by Rosemount Co. The system pressure is measured with DPI 260 model of Druck Co. installed on the reactor vessel upper plenum. The orifice flow meters, equipped in the intact cold legs of each loop, measure the steam flow rate entering downcomer from each intact cold leg. The differential pressure between upper plenum and downcomer is measured with the DP transmitter of Rosemount Co.. The temperatures are measured by T-type

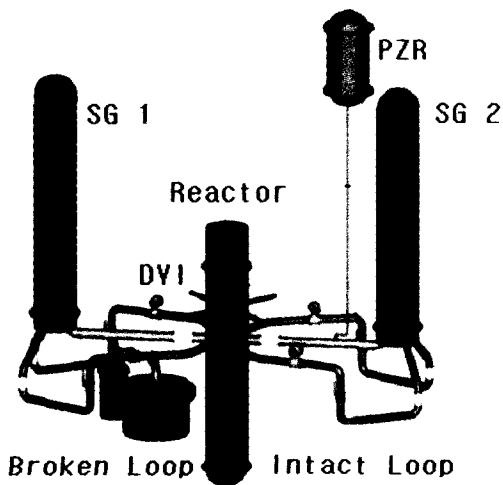


**Fig. 9. Bird's Eye View of SNUF**

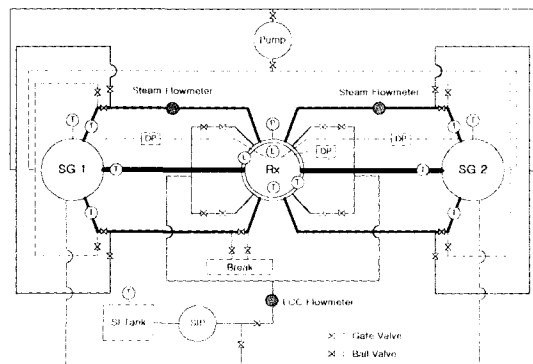


**Fig. 10. Instrument System of SNUF**

thermocouples in upper plenum, downcomer, each cold leg, each hot leg, and each steam generator primary exit.

#### 4. Procedure of Experiment

The structures of the primary system are pre-heated to about 100°C to minimize the heat loss during the test duration. The temperature of secondary system is maintained on saturation condition at 0.2MPa. The core coolant is drained through the drain valve installed underneath the bottom of the reactor vessel until the coolant level falls to the bottom of cold leg. The drain valves, equipped in each suction leg, drain the residing coolant in the pipe. At the start of the test, all the discharge valves are opened and the separation valve is closed simultaneously to simulate the break and the heater power is turned on.

To simulate the actual system behavior of LB-LOCA in the prototype during the steady state duration before start of experiment, heaters have to be maintained power-on and safety injection water is continuously supplied. However, in case that SI water was supplied to downcomer through DVI before start of experiment, SI water suppressed the incoming steam into downcomer due to the low steam velocity and the liquid in the downcomer flowed reverse into the intact cold leg. According to the quantity of the residing coolant in the leg, the thermal hydraulic behavior during transient may be changed through the residing coolant interacting with steam in the leg. To remove the experiment uncertainty, we maintained initial status of heater and SI water differently from the actual before start of experiment.

According to the validation test of experiment sequence change as shown in Figs. 11 and 12, there were some differences in initial behavior of downcomer level. But, during the main test

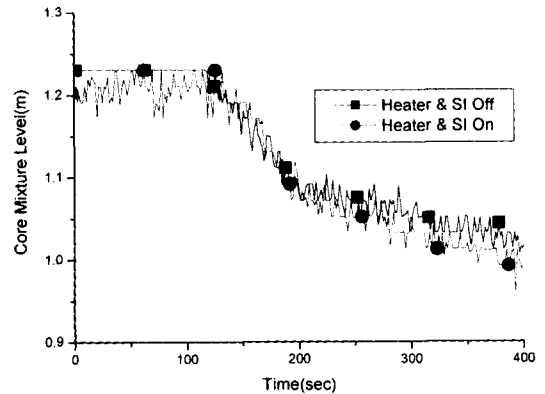


Fig. 11. Core Mixture Level

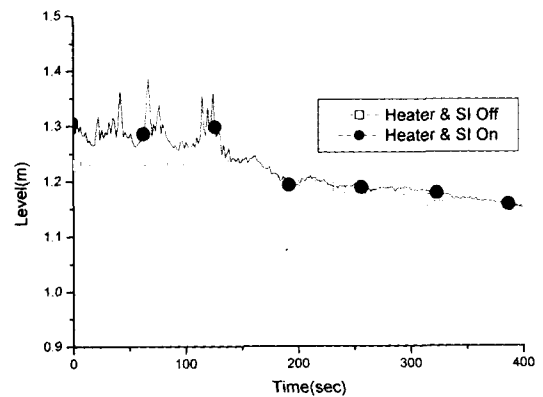


Fig. 12. Downcomer Liquid Level

duration from about 140.0sec, when core two-phase level starts to be depleted by spill-over and sweep-out in addition to evaporation, both cases showed nearly same trends in core two-phase mixture level and downcomer level.

### 5. Experimental Results

#### 5.1. Difference Between Sweep-out and Spill-over

The initial condition of experiment is the plant state of the long-term cooling phase, two hours elapsed from the initiation of LB-LOCA in cold

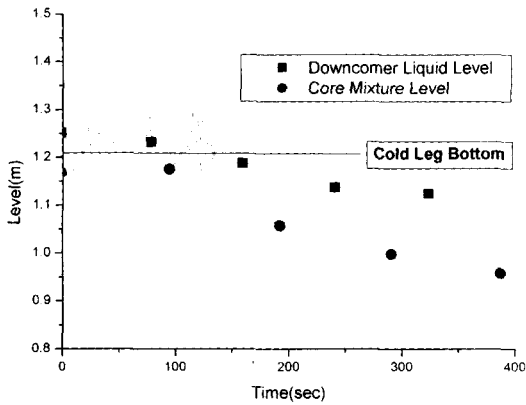


Fig. 13. Core and DC Coolant Level

leg. The SIP continually supplies SI water to downcomer through DVI from the actuation to the failure of SI. When the decay heat decreases, SI water suppresses the incoming steam into downcomer due to the low steam velocity. Since the downcomer liquid level is oscillated by the steam condensation as shown in the Fig. 13, the liquid in the downcomer flows reverse into the intact cold leg. It can refill the loop seal and block the steam passing through the intact cold legs. If the loop seal is open, both sweep-out and spill-over are occurred during transients. On the other hand, if the loop seal is closed, sweep-out is not occurred because the steam cannot enter into the downcomer. We performed experiment for both cases of loop seal open and closed. There are some differences in the behaviors of system between sweep-out and spill-over. The sweep-out phenomenon is that the incoming steam from intact cold leg drags the downcomer water to break as shown in Fig. 14. As the core two-phase mixture level decreases, so the downcomer liquid level decreases. Sweep-out continues to the critical void height below the bottom of cold leg for the given steam flow. On the other hand, spill-over is caused by the differential pressure between the upper plenum and the downcomer. During Spill-

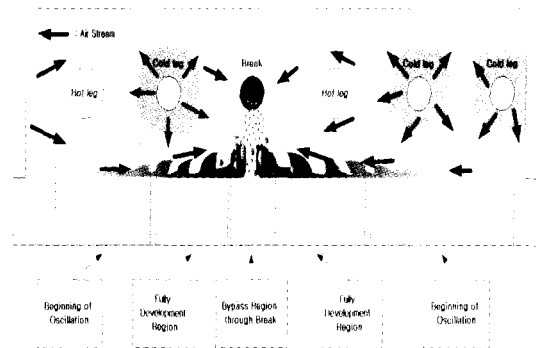


Fig. 14. Sweep-out Phenomenon

over is occurred, the downcomer liquid level is maintained constant to the bottom of cold leg even if the core two-phase mixture level decreases.

### 5.2. Case 1(Loop Seal open)

As the initial conditions of test, the liquid level was maintained close to the bottom of the cold leg and the liquid temperature was maintained about 95°C in the atmospheric pressure to simulate the plant state at two hours after the LB-LOCA initiation. SG secondary side pressure was 0.2MPa. The steady state condition was maintained before starting test.

On turning on the heater power at 100.0sec, the liquid in the core was boiled up to the saturated condition and the swelled-up mixture began to spill-over into both the hot legs at about 120.0sec as shown in Figs. 15 and 16. This spill-over to hot legs reduced the static head in the core so that the liquid in the downcomer surged into the core by the static head difference to lower the water level in the downcomer as shown in Fig. 16. The upper plenum pressure was gradually increased as shown in Fig. 17. The pressure buildup in the upper plenum gave rise to the out-surge of the liquid from the core into the downcomer, which restored the downcomer level up to the bottom of the cold leg and eventually

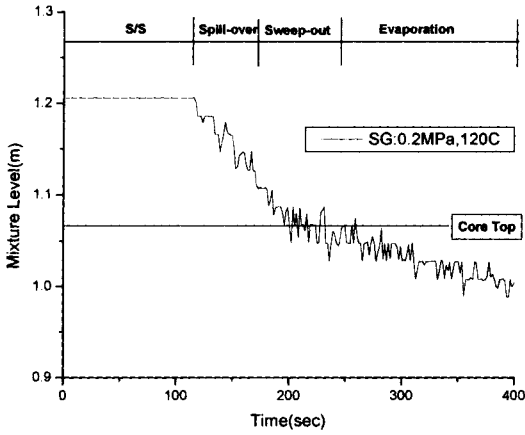


Fig. 15. Core Mixture Level

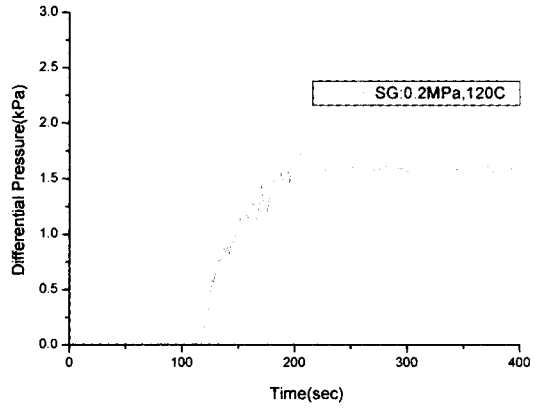


Fig. 18. DP Between UP and DC

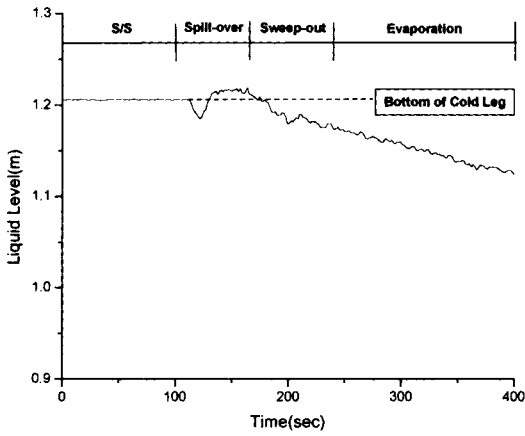


Fig. 16. Downcomer Liquid Level

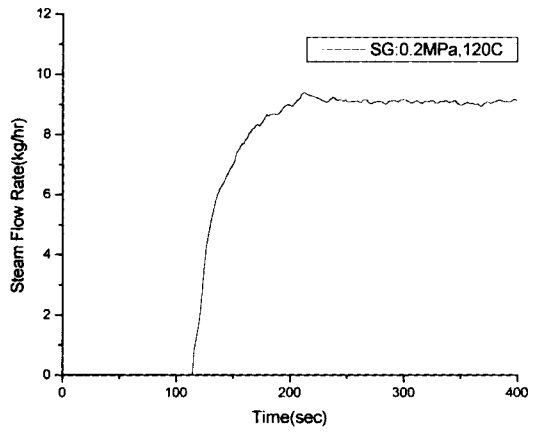


Fig. 19. Steam Flow Rate in Loop 1

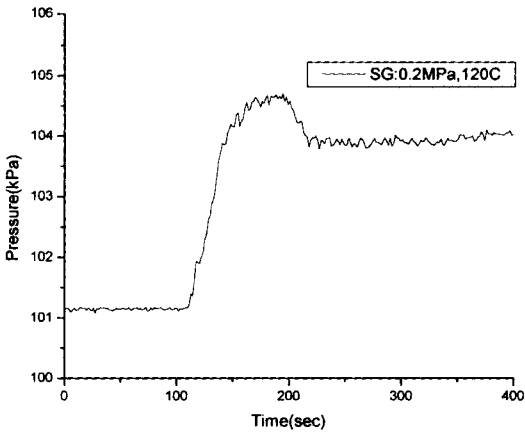


Fig. 17. Upper Plenum Pressure

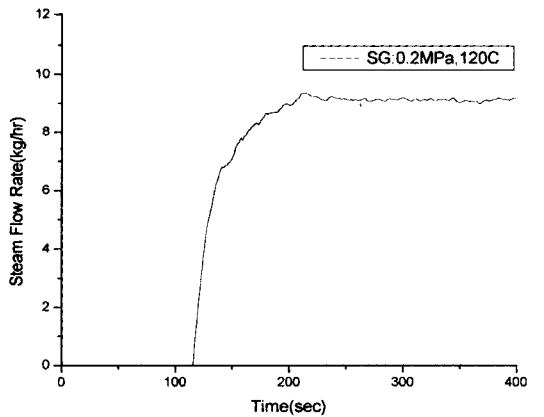


Fig. 20. Steam Flow Rate in Loop 2

generated the spill-over into the broken cold leg at about 140.0sec as shown in Fig. 16. During spill-over was occurred, the downcomer water level was maintained nearly constant but the core level was decreased almost as much as the spill-over from 140.0 to 180.0sec as shown in Figs. 15 and 16. At about 180.0sec, the spill-over to cold leg was terminated when the downcomer water level was lowered below the bottom of the cold leg as shown in Fig. 16.

The differential pressure between upper plenum and downcomer and the steam flow rate increased due to the buildup of the upper plenum pressure as shown in Figs. 18, 19 and 20. After the termination of the cold leg spill-over, the core two-phase mixture level was decreased faster from 180.0sec to about 250.0sec than the latter half of the test as shown in Fig. 15. In the meantime, the downcomer water level was gradually decreased as shown in Figs. 16 on the condition that the steam flow rate through the intact cold leg remained nearly constant as shown in Figs. 19 and 20. This thermal hydraulic behavior may be explained in terms of sweep-out of water in the downcomer. While the steam entering the downcomer from the intact cold leg was gushing above the surface of water in the downcomer, the steam dragged the liquid into the broken cold leg to reduce the

coolant inventory in the reactor vessel and it accelerated the decrease rate of core mixture level. The decrease rates of core mixture level were measured 0.16cm/sec in the former and 0.036cm/sec in the latter. The core two-phase mixture level decreased about 5 times faster in the former half than the latter due to sweep-out.

**5.3. Case 2(Loop Seal Closed)**

In case that the loop seal is closed, the steam from intact cold legs cannot enter into the downcomer. Thus, spill-over dominates the core mixture level without the sweep-out in the downcomer. On the condition of loop seal blocked, the initial conditions such as the liquid level, the core level and the liquid temperature were maintained same with Case 1 of loop seal open.

On turning on the heater power at 100.0sec, the coolant in the core was boiled up to the saturated condition. The upper plenum pressure and the differential pressure between upper plenum and downcomer increased more than Case 1 of loop seal open as shown in Figs. 21 and 22. The core mixture level was rapidly dropped from 115.0sec to 220.0sec as shown in Fig. 23 while the differential pressure between upper

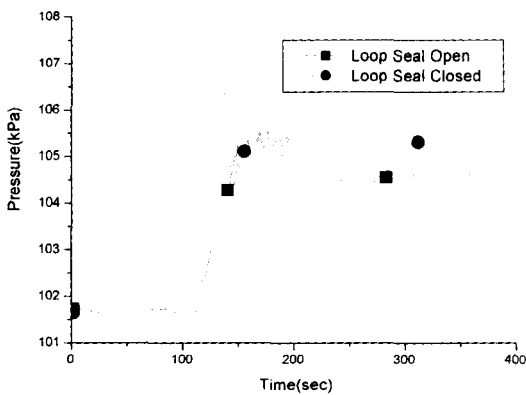


**Fig. 21. Upper Plenum Pressure**

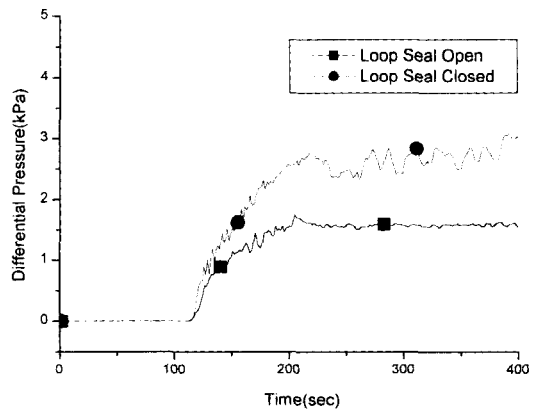


**Fig. 22. Diff. Pr. Btn Upper Plenum & Downcomer**

plenum and downcomer induced spill-over. Meanwhile, the downcomer water level was maintained nearly constant above cold leg bottom as shown in Fig. 24. The larger differential pressure between upper plenum and downcomer made the core mixture level decrease faster than Case 1 of loop seal open. So, it could increase rapidly the discharge flow through the break and induce the abrupt core uncover. Thus, when SI failure is occurred during the long-term cooling phase of LB-LOCA, the status of loop seal has to be observed carefully to mitigate the depletion of core coolant inventory.

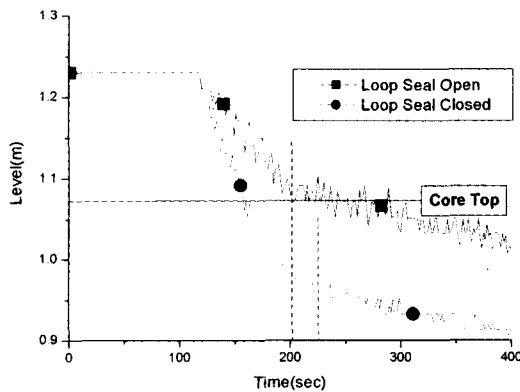


Fig. 23. Core Mixture Level

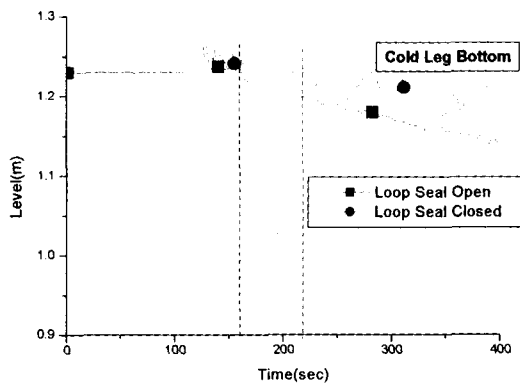


Fig. 24. Downcomer Liquid Level

### 5.4. Comparison of MAAP4.03 and Experiment Results

Test results showed that the depletion of core coolant inventory was accelerated by spill-over and sweep-out in addition to coolant evaporation. However, since MAAP4.03 calculates the thermal hydraulics in the simplified method of considering only mass and energy equations without momentum equation, steam generation rate by the fuel submerged below the core two-phase mixture level determines the decrease of core mixture level without spill-over and sweep-out as shown in Fig. 25. The core two-phase mixture level,  $Z_{wv}$ , is calculated as follows:

$$Z_{wv} = Z_{sub} + \frac{(M_{wcr} - M_{wsub})v_{wcr}}{(1 - \alpha_{cr})A_{cr}} \quad (27)$$

where,  $Z_{sub}$ ,  $M_{wcr}$ ,  $\alpha_{cr}$ ,  $M_{wsub}$ ,  $v_{wcr}$  and  $A_{cr}$  are elevation of subcooled-line, total core coolant mass, core void fraction, coolant mass of subcooled-line, specific volume of core coolant and core flow area, respectively.

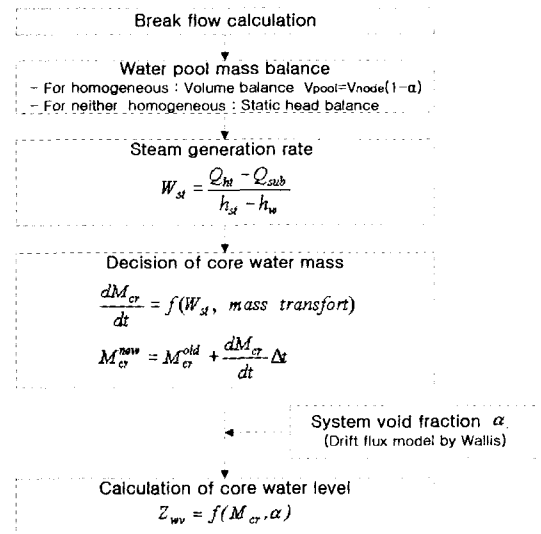


Fig. 25. Core Two-phase Mixture Level Calculation Algorithm in MAAP4.03

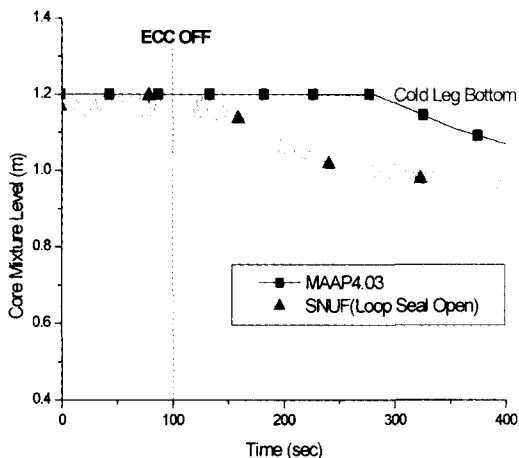


Fig. 26. Core Mixture Levels (Loop Seal Open)

Since the core mixture level takes major role in the fuel heat-up rate, the location of fuel melting initiation and the channel blockage by melting material during SA, we assessed the core coolant inventory calculation model of MAAP4.03 through comparing the calculated of MAAP4.03 with experimental results in the following.

In case of loop seal open, the core two-phase mixture level measured in the experiment indicates that sweep-out and spill-over contribute to decreasing the core mixture level faster than the estimated of MAAP4.03 as shown in the Fig. 26. As illustrated in the Fig. 25, in the calculation of core two-phase mixture level, this code considers only the steam generation by heaters submerged below the core mixture level without including the sweep-out and spill-over. When the downcomer water level came down below the critical void height for sweep-out, the sweep-out was terminated such that the core two-phase mixture level almost linearly decreased from 250.0sec similar to MAAP4.03.

In case of loop seal closed, experiment result shows that the core two-phase mixture level is dropped much more rapidly than MAAP4.03 as shown in the Fig. 27. This difference between

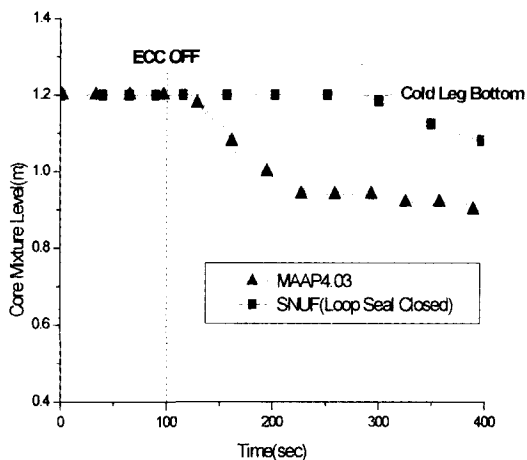


Fig. 27. Core Mixture Levels (Loop Seal Closed)

experiment result and the estimated of MAAP4.03 is originated from that MAAP4.03 does not consider the status of loop seal. Since MAAP4.03 cannot simulate the status that the loop seal is closed, it calculates the differential pressure between upper plenum and downcomer lower than the actual. Thus, the quantity of out-surge from core to downcomer is reduced and the core mixture level is calculated higher than the experiment result.

## 6. Conclusions

This study intended to investigate the depletion of core coolant inventory during transition from DBA to the commencement of SA, which affects the fuel heat-up rate, the location of fuel melting initiation and the channel blockage by melting material during SA. As a part of DBA and SA combined analysis method development research, we investigated experimentally and analytically the depletion of core mixture level during the long-term cooling of LB-LOCA according to the status of loop seal.

In case of loop seal open, the core mixture level decreased about 5 times faster in the former half

than the latter of the transients. This difference of the thermal hydraulic behavior resulted from the sweep-out by the interaction between incoming steam and liquid in the downcomer. MAAP4.03 estimated the core level higher than the measured value because the code did not account for the thermal hydraulic phenomena such as sweep-out and spill-over. When the downcomer coolant level fell below the critical void height for the occurrence of sweep-out, the core mixture level decreased linearly pursuant mostly to evaporation in the core similar to MAAP4.03.

In case of loop seal closed, sweep-out did not occur since the steam could not enter downcomer. In the other side, the differential pressure between upper plenum and downcomer was increased higher than that of loop seal open. Thereby, there was a large out-surge from core to downcomer and the core mixture level was abruptly dropped. Thus, when SI failure is occurred during the long-term cooling phase of LB-LOCA, the status of loop seal has to be observed carefully to mitigate the depletion of core coolant inventory. In the comparison with MAAP4.03, since MAAP4.03 cannot simulate the status that the loop seal is closed, it calculates the differential pressure between the upper plenum and downcomer lower than the actual and the core mixture level is calculated higher than the experiment result.

As a whole, MAAP4.03 overestimates the core two-phase mixture level for both cases during the former half of transients against the conservatism. In order to hold the conservatism in the accident analysis of nuclear plant, it is recommended that the core two-phase mixture calculation of MAAP4.03 should be improved to consider the thermal hydraulic phenomena such as sweep-out and spill-over and the measures to simulate the status of loop seal.

### Nomenclature

|           |   |
|-----------|---|
| $A$       | flow area or flow area ratio                    |
| $a$       | component flow area [mm <sup>2</sup> ]          |
| $c_p$     | specific heat [kJ/K-kg]                         |
| $d$       | hydraulic diameter [mm]                         |
| $E$       | energy [kJ]                                     |
| $f$       | friction factor                                 |
| $g$       | gravitational constant [9.8m/sec <sup>2</sup> ] |
| $i$       | specific enthalpy [kJ/kg]                       |
| $K$       | loss coefficient                                |
| $l$       | component length [m]                            |
| $N$       | dimensionless number                            |
| $p$       | pressure [MPa]                                  |
| $\dot{q}$ | heat generation rate [kW]                       |
| $T^*$     | time ratio number                               |
| $u$       | velocity [m/sec]                                |
| $V_{gj}$  | drift velocity [m/sec]                          |
| $w$       | work [kJ]                                       |
| $x$       | quality   |

### Greek Letters

|          |                                   |
|----------|-----------------------------------|
| $\alpha$ | void fraction                     |
| $\Delta$ | difference                        |
| $\delta$ | conduction depth [m]              |
| $\mu$    | viscosity [N-sec/m <sup>2</sup> ] |
| $\rho$   | density [kg/m <sup>3</sup> ]      |
| $\tau$   | time constant                     |
| $\xi$    | wetted perimeter [mm]             |

### Subscripts

|     |                 |
|-----|-----------------|
| 0   | reference       |
| e   | exit            |
| f   | liquid or fluid |
| g   | gas or vapor    |
| i   | i-th component  |
| m   | model           |
| p   | prototype       |
| R   | ratio           |
| sub | subcooling      |



### References

1. "RELAP Code Manual", U. S. Nuclear Regulatory Commission, Washington, USA, (1999).
2. P. Hofmann, "Current knowledge on core degradation phenomena, a review", Journal of nuclear materials, (1999).
3. "Standard Safety Analysis Report for the Korean Next Generation Reactor", Korea Electric Power Corporation, Seoul, Korea, (1999).
4. Hong, S.J. and Park, G.C., "Study on Post-Blowdown of Hot-Leg Large Break Loss-of-Coolant-Accident in the View of Mass and Energy Release Analysis", Nuclear Engineering and Design, (2001).
5. Ishii, M. and Kataoka, I., "Scaling Laws for Thermal Hydraulic System under Single Phase and Two Phase Natural Circulation", Nuclear Engineering and Design, (1984).
6. Yun B.J. et al., "Development of Scaling Law for the Direct ECC Bypass during LB-LOCA Reflood Phase with Direct Vessel Injection System", Proceedings of the Korean Nuclear Society, (2000).
- 7 "MAAP4.03 User' s Guide", Electric Power Research Institute, Palo Alto, CA, USA, (1994).
8. "MARS2.1 Code Manual", Korea Atomic Energy Research Institute, Taejon, Korea, (2002).
9. Tong, L.S., "Boiling Heat Transfer and Two Phase Flow", Wiley and Sons, Inc., New York, NY, USA, (1965).
10. " Flow of Fluids through Valves, Fittings and Pipe", CRANE, New York, USA, (1985).
11. " Decay Heat Power in light water reactors", ANSI/ANS 5.1-1979, ANS, USA, (1979).